(12) INTERNATIONAL APPLICATION PUBLISHED UNDER THE PATENT COOPERATION TREATY (PCT)

(19) **World Intellectual Property Organization**
International Bureau

(43) **International Publication Date**
19 January 2012 (19.01.2012)

PCT

(10) **International Publication Number**
WO 2012/007061 A1

(51) **International Patent Classification:**
H04N 9/04 (2006.01) ***H04N 5/357*** (201 1.01) ***H04N 9/07*** (2006.01)

(21) **International Application Number:** PCT/EP2010/060367

(22) **International Filing Date:** 16 July 2010 (16.07.2010)

(25) **Filing Language:** English

(26) **Publication Language:** English

(71) **Applicant** *(for all designated States except US):* **ROBERT BOSCH GMBH** [DE/DE]; Postfach 30 02 20, 70442 Stuttgart (DE).

(72) **Inventors; and**
(75) **Inventors/ Applicants** *(for US only):* **SCHIRRIS, Johan** [NL/NL]; Pietershoek 46, NL-5503 XA Veldhoven (NL). **CVETKOVIC, Sasa** [NL/NL]; Joh van der Waalsweg 100, NL-56 12 JD Eindhoven (NL).

(74) **Common Representative: ROBERT BOSCH GMBH;** Postfach 30 02 20, 70442 Stuttgart (DE).

(81) **Designated States** *(unless otherwise indicated, for every kind of national protection available):* AE, AG, AL, AM, AO, AT, AU, AZ, BA, BB, BG, BH, BR, BW, BY, BZ, CA, CH, CL, CN, CO, CR, CU, CZ, DE, DK, DM, DO, DZ, EC, EE, EG, ES, FI, GB, GD, GE, GH, GM, GT, HN, HR, HU, ID, IL, IN, IS, JP, KE, KG, KM, KN, KP, KR, KZ, LA, LC, LK, LR, LS, LT, LU, LY, MA, MD, ME, MG, MK, MN, MW, MX, MY, MZ, NA, NG, NI, NO, NZ, OM, PE, PG, PH, PL, PT, RO, RS, RU, SC, SD, SE, SG, SK, SL, SM, ST, SV, SY, TH, TJ, TM, TN, TR, TT, TZ, UA, UG, US, UZ, VC, VN, ZA, ZM, ZW.

(84) **Designated States** *(unless otherwise indicated, for every kind of regional protection available):* ARIPO (BW, GH, GM, KE, LR, LS, MW, MZ, NA, SD, SL, SZ, TZ, UG, ZM, ZW), Eurasian (AM, AZ, BY, KG, KZ, MD, RU, TJ, TM), European (AL, AT, BE, BG, CH, CY, CZ, DE, DK, EE, ES, FI, FR, GB, GR, HR, HU, IE, IS, IT, LT, LU, LV, MC, MK, MT, NL, NO, PL, PT, RO, SE, SI, SK, SM, TR), OAPI (BF, BJ, CF, CG, CI, CM, GA, GN, GQ, GW, ML, MR, NE, SN, TD, TG).

Published:

— *with international search report (Art. 21(3))*

(54) **Title:** METHOD FOR LATERAL CHROMATIC ABERRATION DETECTION AND CORRECTION

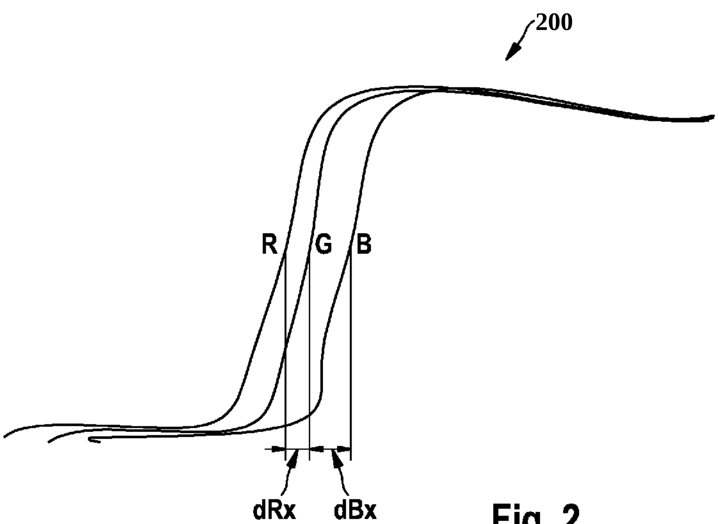

Fig. 2

(57) **Abstract: A** method for detection (10) and correction (40) of a lateral chromatic aberration shift of at least one of a red (R) and a blue (B) color plane in relation to a green (G) color plane in digital image data includes, for at least one region of the digital image data, determining (3) a first edge in the red (R) and/or blue (B) color plane; determining (3) a second edge in the green (G) color plane or in a color plane (GonR, GonB) derived (1) from the green (G) color plane, the at least one second edge corresponding to the at least one first edge; determining (6) a shift between the first and second edges; and correcting (40) the lateral chromatic aberration shift by shifting the red (R) and/or blue (B) color plane of the image region.

WO 2012/007061 A1

Description

Title

Method for Lateral Chromatic Aberration Detection and Correction

The current invention relates to a method for lateral chromatic aberration detection and correction, to a corresponding optical image processing device and to a corresponding computer program product.

Prior Art

Chromatic aberration (CA), achromatism or chromatic distortion is a defect of optical lenses in connection with focusing all colors to the same convergence point at a certain distance of the lens (axial or longitudinal chromatic aberration) and/or at a certain location in the focal plane (transverse or lateral chromatic aberration). Both types of aberration are caused by different refractive indices of lenses for different wavelengths (dispersion).

Chromatic aberration is evident from images in form of color fringes along boundaries separating dark and bright areas (edges). The visual effects of longitudinal and lateral chromatic aberration are different in that longitudinal chromatic aberration causes fringes in all places in the scene, whereas lateral chromatic aberration affects objects stronger if they are farther from the center. Fringes caused by lateral chromatic aberration, in contrast to those due to longitudinal chromatic aberration, are typically absent in the image center (typically coinciding with the lens center) and progressively increase toward the image corners.

The performance of color separation, involved in digital image processing, is strongly affected by lateral chromatic aberration and the resulting misalignment of the different color planes.

Chromatic aberration can be reduced or eliminated by using achromatic and apochromatic lenses comprising glasses with different dispersion. However, such lenses are heavy and expensive. A reduction of chromatic aberration by stopping down lenses is, especially in case of lateral chromatic aberration, not always practicable, desired or effective.

Methods for reducing lateral chromatic aberration, hereinafter referred to as LCA, are known from US 2008/0284869 A1, US 7,221,793 B2, US 2008/0291447 A1, US 6,747,702 B1, US 7,227,574 B2, US 2009/0052769 A1, US 7,577,292 B2, US 2007/0242897 A1, US 7,346,210 B2, US 7,142,238 B1, JP 2002 320237 A, US 7,425,988 B2, JP 2000 299874 A, US 2008/0007630 A1, US 7,466,495 B2, US 2008/0062409 A1 and US 7,356,198 B2.

The prior art methods, however, have significant disadvantages. In some cases, pre-calculated LCA model parameters for a certain lens type in the form of a look-up table are used to correct LCA artifacts. These methods are thus limited to the specific lens described by the look-up table. Other prior art documents just disclose LCA correction without taking into account the specific characteristics of lens and LCA present and thus may under- or overcorrect artifacts. In some cases, specific artifacts, referred to as "purple fringing", are targeted, regardless of their origin, in form of a post-processing step. Typically, the prior art methods are not suitable to correct the resolution losses caused by LCA.

Thus, a need for improved ways for detecting and correcting lateral chromatic aberration exists.

Disclosure of the Invention

According to the invention, a method for lateral chromatic aberration detection and correction, a corresponding optical image processing device and a corresponding computer program product according to the independent claims is provided. Preferred embodiments are the subject of the dependent claims and of the description.

Advantages of the Invention

In contrast to the prior art, the current invention includes providing an LCA model to estimate LCA magnification or shift parameters *caR* and *caB,* corresponding to a chromatic aberration shift of the red (in the following referred to as "R") and blue ("B") color plane or component with respect to the green ("G") color plane or component with sub-pixel accuracy, from an arbitrary input image. The method does thus not require use of a reference image known in advance. Based on an edge detection method and including a detection of zero crossings of the red and blue color signals, LCA correction is performed with the LCA parameters thus determined to remove LCA deformations from the image.

Further advantages and embodiments of the invention will be evident from the description and the accompanying drawings. It should be noted that the features mentioned above and to be explained below are not limited to the indicated combinations but are likewise usable in other combinations or alone without departing from the scope of the current invention.

The invention is illustrated by embodiments in the drawings and will be described with reference to the drawings.

Figures

Figure 1 schematically illustrates a Bayer grid according to the prior art.

Figure 2 illustrates an horizontal edge of a color signal including an LCA shift.

Figure 3 illustrates a radial LCA shift of a pixel of a R color plane.

Figure 4 illustrates a radial LCA color shift of a R color plane in an image.

Figure 5 illustrates a radial LCA color shift of a B color plane in an image.

Figure 6 illustrates a method for LCA detection and correction according to a preferred embodiment of the invention.

Figure 7 illustrates a method for LCA detection according to a preferred embodiment of the invention.

Figure 8 illustrates a method of detecting position of an edge of a color signal according to a preferred embodiment of the invention.

Figure 9 illustrates a method of calculating a correction factor according to a preferred embodiment of the invention.

Figure 10 illustrates details of calculating a correction factor according to a preferred embodiment of the invention.

Figure 11 illustrates the restriction of an LCA determination to an image area according to a preferred embodiment of the invention.

Figure 12 illustrates a method of calculating an LCA shift according to a preferred embodiment of the invention.

Figure 13 illustrates a method of calculating an edge position with sub-pixel accuracy according to a preferred embodiment of the invention.

Figure 14 illustrates a bilinear interpolation on a pixel grid according to a preferred embodiment of the invention.

Figure 15 illustrates a method of determining a shift vector according to a preferred embodiment of the invention.

In Figure 1, an image sensor 100 in form of a Bayer grid sensor as frequently used in digital image recording and/or processing devices is shown. It should be noted that, even if the current application is exemplified with a Bayer grid sensor, the methods described herein are equally useful with other types of image sensors including grids wherein different color pixels are recorded at different locations. In the sensor 100, the R, G (in form of G1 and G2) and B pixels are placed in a so-called Bayer pattern.

As the different colors are recorded at different locations (pixels), a color separator is required to interpolate (find an estimate) of R, G and B values at the current pixel on a position (x, *y)* by using existing samples in the neighborhood of the current location. This image "reconstruction" to a full resolution can only be performed satisfactorily if all three image planes are well aligned, i.e. when no shift exists between them. However, lateral chromatic aberration misaligns color planes and thus reduces the performance of the color separator.

An example of LCA is presented in Figure 2, where a horizontal edge 200 in an image including a horizontal (x) color shift of the R and B color planes *(dRx, dBx)* is shown. A similar effect can also be noticed in the vertical *(dRy, dBy)* or any other direction. For the following discussion, *r* shall represent a radial distance of the current pixel from the center of the sensor (typically coincident with the center of the lens) and *caR* and *caB* are parameters of the LCA model for the R and B color planes respectively. In the following description, these two parameters will also, commonly, be referred to as *caRB.*

LCA misalignment can be modeled by a 3rd order polynomial:

$$f(r) = caRB_3 * r^3 + caRB_2 * r^2 + caRB_1 * r^1 + caRB_0.$$

For reasons of robustness and easier parameter estimation, this function can be simplified to a first order polynomial form

$$f(r) = caRB * r.$$

A crucial aspect of the current invention is the determination of the *caRB* parameters. The function *f(r)* describes a shift of the R and B pixels with respect to the (reference) G pixel and is depicted as a shift vector *(dRx, dRy)* in Figure 3. As can be seen from Figure 3, the "real" values of the R or B pixels on any position (x, *y)* are not the ones that are measured on that position but are displaced to a new location given by the shift vector. This new position is usually not located on the existing pixel grid, so the real pixel's value has to be estimated from its neighbors k, l, m and n.

LCA color shifts in an image with 25 * 25 pixels are exemplified in Figure 4 (for the R plane) and Figure 5 (for the B plane). It can be noticed that shifts are approximately zero in the image center and that they increase in their absolute value towards the image edge. In most cases, if the G color plane is taken as a reference, the shift of the R color plane has a direction opposite to the shift of the B color plane. As evident from Figures 4 and 5, the resulting effect is equivalent to a "magnification" of the R color plane and a "shrinking" of the B color plane.

The steps of the zero-crossing based detection method according to an embodiment of the current invention are schematically shown in Figure 6. The current invention includes detecting 10 LCA directly from the image and estimating or determining 20 the LCA magnification parameters *caR* and *caB.* A LCA parameter calculation method is employed which directly estimates the LCA shift from the image data, based on the detection of zero-crossings. After estimation of the parameters, and after a reliability check 30, LCA correction 40 is performed via re-sampling the R and B color planes.

Input to the methods of the invention are R, G and B color planes originating, e.g., from a Bayer pattern sensor as in Figure 1. The LCA shift between the G and R (or B) color channels is measured by matching corresponding edges in these color channels and by calculating their distances *(dRx, dRy, dBx* and *dBy,* cf. Figure 2) with sub-pixel accuracy. For this purpose, an edge detection for all three color channels needs to be performed and the edge distances between the R and the G as well as the B and the G color channel need to be determined. However, due to the color planes originating, e.g., from a Bayer grid, the values of the R, G and B color pixels on each location are not directly available. Therefore, when estimating LCA shifts, one has to correct for a total color plane shift to enable a correct matching.

For this purpose, e.g., lists *LCA_R* and *LCA_B* of relevant data for all edge pixels which are taken for the LCA detection are generated. For instance, the first two columns of such lists are the line and the pixel number of the edge pixel and the third column is a detected shift (which can be positive, negative or zero).

The overall steps of LCA detection are set forth below and illustrated in Figure 7. Essentially, these steps include recalculating 1 the G color samples on the R and B Bayer grid position, low-pass filtering 2 the color planes as preparation for the edge detection, edge detection 3 using a Laplacian operator and a set of conditions, calculating 4 a correction factor for an edge shift, a check 5 whether the detected edge pixels satisfy a set of conditions, calculating 6 a LCA shift between color planes with sub-pixel accuracy and generating 7 a list of data for detected edge pixels, marking their position and LCA shift.

As mentioned above, a correct matching of edges originating from three color planes needs to be performed. For this matching to be feasible, G color samples can be recalculated 1 (see Figure 7) to correspond to the R and B pixel positions. These new color planes will be referred to as GonR and GonB. A second option is to correct for the edge shift that is equal to 0.5 pixels during calculation of the edge shift. For instance, for calculation of the horizontal edge shift between the G and B color planes, an edge detection on the G2 (cf. Figure 1) pixels and, in the vertical direction, on the G1 pixels may be performed. Similarly, for calculation of the horizontal edge shift between the G and R color planes, an edge detection on the G1 pixels and, in the vertical direction, on the G2 pixels may be performed.

If, for example, an edge is detected in the horizontal direction (vertical edge) on the B color plane on a position $(x, y) = (2, 2)$ relative to the B color plane (with an absolute position on Figure 1 of $(x, y) = (3, 3)$), the edge should be at a position of $(x, y) = (1.5, 2)$ on the G2 color plane, provided no edge shift between the G and B color planes exists. This 0.5 pixel shift needs to be corrected in the further calculations. Similar arguments hold for edges detected in a vertical direction, as well as for the detection of edge shift between the R and G color planes. For the ease of explanation, position corrected G color planes that are used for color shift detection will be referred to as GonR and GonB color planes.

As mentioned above, a low-pass filtering 2 (cf. Figure 7) of the R, B, GonR and/or GonB color planes is performed as preparation for the edge detection. Edge positions should be detected with sub-pixel accuracy on all color planes. Edges can, in the context of the current application, be detected, e.g., by means of a Sobel or Canny or any other edge detector. Many of the known methods, however, do not produce one pixel wide edges. Therefore, consecutive edge tinning must be applied. However, with 1st order high-pass filters it may be difficult to find a sub-pixel accuracy position of the edge.

Therefore, preferably edge detection is performed including filtering 3 to improve the noise robustness (cf. Figure 7) using a second order high-pass filter (e.g., a Laplacian filter [-1 2 -1]) which has zero output on the position of an edge. Furthermore, advantageously several test criterions are checked. Separate calculations for the horizontal and vertical direction need to be performed to reduce the influence of neighboring edges on the edge detection and the position of the edge. The Laplacian operator is generally rather noise sensitive, which is why it is advantageously combined with a Gaussian low-pass filter in the same direction as a high-pass filter part. This operator is also referred to as Laplacian of Gaussian (LOG) and is in fact a band-pass filter with better noise suppression. For extra noise robustness, prior to LOG filtering, a low-pass filter can be applied in the direction opposite to the main filtering direction. Instead of applying a LOG filter with a pre-filtering operation in the opposite direction from the edge detection operation, also a 2D low-pass filtering and then a simple Laplacian filtering operation may be performed.

As stated, this operation is advantageously performed for robust and accurate edge detection, however, it is equally beneficial for the line-angle detection operation (described below) where a 1st order high-pass filter is used. For example, a 2D low-pass filter that can be advantageously used for filtering all color channels (R, GonR, GonB and B) is given by

$$LP = \frac{1}{16}\begin{vmatrix} 1 & 2 & 1 \\ 2 & 4 & 2 \\ 1 & 2 & 1 \end{vmatrix}.$$

As a further step 3 (cf. Figure 7), as noted above, candidate edges for further processing are to be determined. As previously explained, a Laplacian filter [-1 2 -1] will be applied on all color planes, separately in the horizontal and vertical direction. However, advantageously only such types of edges should be taken into account which enable a good and correct detection of the LCA shift. Such edges advantageously include isolated edges with sufficient magnitude (dynamic range).

In Figure 8, an edge of one of the four color signals, generically referred to as "C" (C = R, GonR, GonB and B), is shown at and between four pixel positions (samples), px-1 , px, px+1 and px+2. In Figure 8, the high-pass output of the Laplacian filter is shown in form as a signal *hp.* The real position E of the edge of the signal C is usually not positioned on one of the pixels px-1 , px, px+1 and px+2, and can be determined by the zero crossing. To define a sub-pixel position of the edge, a reference point P of the edge pixel found with a pixel accuracy on the position px is used. The value Δ indicates the sub-pixel position of the zero crossing (i.e., the distance between the real edge position E and the position P of the detected edge pixel). While crossing zero, the sign 800 of the *hp* signal changes its value, for example, from - to +.

If an adequate, isolated edge with sufficient dynamic range is to be detected, advantageously the following condition set is applied:

$$hp(px-1)\ ^{*}\ hp\{px) \geq 0\ \&\&$$
$$/?p(px+1)\ ^{*}\ hp\{px+2) \geq 0\ \&\&$$
$$hp\{px)\ ^{*}\ hp(px+1) < 0\ \&\&$$
$$\backslash\ (C(px) - C(px+1))\ \backslash > TH.$$

In other words, two samples on the left of the edge zero-crossing and two samples on the right of the edge zero-crossing should have the same sign, while *hp* changes sign between the two middle samples. Furthermore, the edge height needs to be larger than a threshold *TH.* A check on the edge size is performed on the image itself, not on the high-pass signal. *TH* can be a constant, but may equally depend from the global contrast in the image or even on a local contrast. The step of applying the condition set on the detected edges is performed separately in the horizontal and vertical direction for all four color planes. Detection in the diagonal direction is also advantageous but more complex.

In a next step 4 (cf. Figure 7), a correction factor (CF) is calculated. To illustrate the principles of calculating CF, in Figure 9 a detected edge on the GonR (see above) color channel and its corresponding edge detected in the R color channel is shown in a quadrant of an image with an image center at *(Xc, Yc).* To describe the LCA shift, a distance between R and GonR (the G color plane at the R position) is to be calculated (see also Figure 2). The distance calculation should (cf. Figures 4 and 5) most advantageously be performed in the radial direction 900, resulting in a distance *d*. However, this operation is challenging to be performed correctly. For this reason, the distance *d* between the lines is measured in the horizontal *dx* or vertical *dy* direction, depending on the edge direction. However, the radial distance of two edges (distance *d* between points A and B in Fig. 9) is not equal to their horizontal distance (distance *dx* between A and C in Figure 9) or vertical distance (distance *dy* between A and D in Figure 9).

Therefore, a conversion has to be applied to correct this discrepancy, which is performed by using a correction factor (CF). CF depends on two angles, namely the pixel angle Θ and an edge angle a. Angles are defined counter-clockwise, starting from the positive direction of the x-axis, where the x-axis and the y-axis pass trough the image center *(Xc, Yc).* The Angle Θ (in Figure 9) represents an angle of the current pixel with respect to the image center. It is in the range from 0 to 2ττ. a is an angle of the considered edge trough that pixel and is in the the range from 0 to ττ.

To derive an exact formula for CF, it should be noted that the edge pixel denoted A in Figure 9 will be shifted in the R (or B) color plane to a position B in the radial direction (in the following, a shift outwards will be assumed and assigned a positive sign). The shift distance is *d*. The shift is measured in the horizontal and in the vertical direction. A search is performed in the horizontal direction around pixel A and a pixel D will be found in a distance *dx.* Similarly, in the vertical direction, a pixel C will be found in a distance *dy.* However, we must realize that found edge pixels C and D originate from pixels A_1 and A_2 from the edge line in the G color channel, respectively, and not from the considered edge pixel A. As long as pixels A, A_1 and A_2 are collinear, this does not represent a problem, but if they do not lie not on the same line, the pixels C and D are falsely determined, and, thus, this edge pixel has to be ignored.

Figure 10 includes further details when compared with Figure 9. The left part of Figure 10 largely corresponds to Figure 9 whereas the right part of Figure 10 shows an enlarged portion of the shaded region in the left part of Figure 10. From Figures 9 and 10 it can be noted that *CF* is a factor that transforms a shift measurement performed in a horizontal *(dx)* or vertical *(dy)* direction to the (radial) direction. This factor is different in the horizontal and vertical direction, so *CFx* and *CFy* are different:

$$d = dx * CFx = dy * CFy.$$

CFx can be derived as follows (cf. Figure 10, right part):

$$D = dx * \mathbf{sin(TT-} a) = d * \sin(n - (a - \Theta)) \rightarrow$$
$$dx * \sin(a) = d * \sin(a - \Theta) \rightarrow$$
$$d = dx * \sin(a)/\sin(a - \Theta) \rightarrow$$
$$CFx = \sin(a)/\sin(a - \Theta).$$

Correspondingly, *CFy* can be derived as follows (cf. Figure 10, right part):

$$D = dy * \sin(a - \tau\tau/2) = d * \sin(n - (a - \Theta)) \rightarrow$$
$$dy * \cos(a) = d * \sin(a - \Theta) \rightarrow$$

$$d = dy * \cos(a)/\sin(a - \Theta) \rightarrow$$
$$CFy = \cos(a)/\sin(a - \Theta).$$

Since only the modulo and not the sign of *dx* and *dy* should be changed by *CF*, *CF* is defined advantageously with an absolute value so that it is valid for all four quadrants of the angle Θ and all angles a. Hence,

$$CFx = |\sin(a)/\sin(a - \Theta)|,\ CFy = |\cos(a)/\sin(a - \Theta)|.$$

In a next step 5 (cf. Figure 7), a check is performed whether detected edge pixels satisfy a set of conditions. For successful operation, the detected edge should be an isolated one to ensure that we the same edge is matched in different color planes. Hence, for example, around the current GonR edge pixel there should to be no other detected edge in the GonR color plane. Otherwise, a detected R edge could be matched with the wrong edge in GonR. This search should be advantageously performed in a consistent manner and isolated edge pixels should be ignored. Therefore, one has to check for a set of conditions (which will be explained in the following regarding the example of the R color plane but are equally valid for the B color plane):

1) an edge at the current GonR pixel exists;

2) no edges on the same horizontal (or vertical) line within the search area around the current GonR edge pixel exist;

3) only one edge in the R color plane within the search area exists;

4) at least one extra edge pixel in the upper or lower line exists which is 8-connected with the current edge pixel (is within the 3x3 window around the current pixel);

5) the *hp* signal in GonR changes its sign (zero crossing);

6) edges in GonR and in R color planes should be similar; for instance they should look like each other and have similar size. They should be of the same type (have the same sign of the second pixel out of four considered pixels around an edge). Consequently, measurement of luminance edges is preferred over color edges;

7) for edge checking in horizontal direction, the edge angle a (Figure 9) should be between $\pi/4$ and $3\pi/4$; for the vertical direction, the angle a should be between $[0 \ldots \pi/4]$ or $[3\pi/4 \ldots \pi]$; furthermore, the edges in the R and GonR as well as in the B and GonB color planes should have a similar angle a to insure the same edge is matched,

8) the correction factor CF is between TH_1 (for instance 0.5) and TH_2 (for instance 2); the larger or the smaller the CF, the more error is introduced to the LCA measurement, so such edge pixels will be skipped;

9) the LCA shift according to its simple model is linearly dependent on the radial distance of the pixel from the image center: $f(r) = d = caRB * r$. For small radial distances, this shift is very small and can not be estimated well, since mainly noise will be measured. To prevent this, it is preferred not to perform any measurement close to the image center, i.e. for $r < r_0$, where, for instance, $r_0 = 0.2D$, where D is the length of a half diagonal of the image (Figure 11). r_0 can also set as depending on the maximum expected LCA shift and to a value where, for instance, the absolute value of the LCA color shift equals half a pixel. As a simplification, to decrease complexity of calculating the acceptance mask *M*, a rectangle can be used (small rectangle in Figure 11). In this case, the acceptance condition is that the current pixel coordinates (x, y) satisfy the criteria

$$|x - Xc| > r_0 \ OR \ |y - Yc| > r_0,$$

where OR represents a logical or function, |.| represents an absolute value and (Xc, Yc) are coordinates of the center of the image;

10) small LCA measured shifts should be ignored, since such an accuracy can not be achieved; also, the total LCA shift should be smaller than the presumed maximum shift in pixels (lens dependent);

11) purple fringing caused by blooming and saturated image signals (streaking) can be confused for a LCA effect. A solution for this problem advantageously includes to exclude all measurements in the neighborhood of very bright pixels. Likewise, all pixels in ($-\delta, \delta$) neighborhood of the bright pixel in both horizontal and vertical direction may be excluded.

If all of these conditions are not satisfied, the current GonR edge pixel is skipped.

The search area is a parameter that depends on a lens, a radial distance from the image center and an edge angle. By examining the LCA model formula $f(r) = caRB * r$, one can notice that a lens of lower quality and especially wide angle and zoom lenses have larger *caRB* parameters, resulting in larger color shift, spanning more than four pixels at the image corners. Also, the color shift increases with the radial distance from the center. Finally, in case when $dx > d$ or $dy > d$ ($CF < 1$, cf. Figures 9 and 10), one has to extend the search area by dividing it with *CF*. In this way, the search area can be made adaptable. If characteristics of the used lens are unknown, one can, e.g., assume that the maximum shift of LCA is *n* pixels. However, if too large maximum shift is allowed in the calculations, this might result in a situation wherein the edge detection algorithm can not find enough reliable edges in natural scenes.

Therefore, an optimal value of *n* can be determined in a loop, starting with a larger *n* and, depending on the results (sufficient amount of detected edges and a reliable measurement), leaving it as it is or starting to reduce it. If a real maximum shift of LCA is larger than the value of *n* used, serious errors are introduced in the measurement since pixels could be matched which belong to different edges (objects). If blue and red shift are always of the opposite sign, as well as if the direction of the shift is known (for instance, the shift of red always is directed out from the center and blue shift towards the center), the algorithm may be improved since one knows in advance in which direction to search for corresponding edges and completely disregard the opposite direction.

In step 6 (cf. Figure 7), an LCA shift between R, GonR, GonB and B color planes is calculated. Four pixels which are used for the detection of the edge position are /?p(px-1), *hp(px), hp*(*px*+1*)* and *hp(px+2)* are illustrated in Figure 12. If an edge on a GonR or GonB color channel is detected on a position *px,* the real sub-pixel edge position is at a position of $px + \Delta_T$, $\Delta_T < 1$, on a corresponding grid. Δ_1 is a sub-pixel distance from the second pixel to the zero crossing in the GonR (or GonB) color plane. One also notices in Figure 8 that two middle pixel values *hp(px)* and *hp*(*px*+1*)* have an opposite sign.

Assuming that an edge pixel was detected in the GonR color plane and a corresponding edge in the R color plane, and further assuming that these satisfy a set of conditions given in the previous paragraph, their mutual distance in a horizontal or vertical direction, corrected with the corresponding correction factor *CF* represents their sub-pixel accuracy shift. *CF* is a factor that transforms a shift measurement performed in a horizontal or vertical direction to the radial direction, so the real LCA is given as $d = dx * CFx = dy * CFy$. This variable is called *CF,* for both horizontal and vertical direction. The variables *dx* and *dy* are depicted in Figure 12 as *dRx* and *dRy.*

Finally, the LCA shift vector is given as $CF * (\Delta - \Delta_1 + \Delta_2)$ on a R (or B) color grid (see Figure 12). On a full image grid (full Bayer grid sampling frequency), this distance is two times larger. Hence, a candidate edge pixel was recorded with its coordinates (line and pixel number) and a value of the lateral chromatic aberration (shift between color planes) calculated in units of pixels on the R or B color plane.

As a further step 7 (cf. Figure 7), a sub-pixel accuracy edge position depicted with Δ_1 (θr Δ_2) iη Figure 12 is calculated. This can be achieved for instance using an interpolation technique of the prior art and by finding a place where this curve passes trough zero. In Figure 13 an example of the high-pass signal *hp,* shown with four pixels around the zero-crossing position is shown. Values of this signal are hp(px-1) = A, $hp(px)$ = B, $hp(px+1)$ = C and $hp(px+2)$ = D. A linear interpolation is a very simple and advantageous form of interpolation which takes into account only two neighboring pixels (*px* and px+1). Using the similarity of triangles, one obtains the relationship $B / \Delta_1 = C / (1-\Delta_1)$, yielding a value 130 for the distance of the zero-crossing (distance to the position of an edge) from a pixel *px*, $\Delta_1 = B/(B-C)$ at a position close to its real value x.

A better (and more complex) approximation of a real edge position can be achieved using, for instance, a cubic interpolation. This interpolation technique uses all four neighboring pixels and approximates a function between the points *px* and px+1 by a 3rd order polynomial $y(x) = a_0 * x^3 + a_1 * x^2 + a_2 * x + a_3$, where a_0, a_1, a_2 and a_3 are polynomial coefficients that can be derived from values A, B, C and D and x is the position between points px and px+1 at which the interpolated function value is to be calculated. The polynomial coefficients are equal to: $a_Q = D - C - A + B$, $a_1 = A - B - a_Q$ $a_2 = C - A$ and $a_3 = B$. A position x is to be found at which interpolation value y(x) yields a value equal to zero (zero-crossing point). Here, an analytical solution is complex to be found directly, so advantageously values $|y(x)|$ starting from x = 0 (at point px) to x = 1 (at point px+1) are calculated with a certain step and a position x is found that gives a minimum value of the approximation. For instance, a step of 0.1 can be taken, which represents a target sub-pixel accuracy of 0.1. The value of x found, giving a minimum value of $|y(x)|$, is a good approximation of Δ_1 for the GonR edge and Δ_2 for the R edge (from Figure 12).

According to the discussion above, LCA can be seen as different magnification of the R and B color planes. The parameter *caR* represents a magnification of the R color plane and *caB* of the B color plane. *caR* and *caB* are used afterwards to construct shift vectors of each R (or B) pixel with respect to the G pixel. Real magnification is equal to 1 + *caRB* (*caRB* representing both *caR* and *caB* LCA parameters). If, e.g., *caRB* = 0.01, pixel shift for a certain pixel is equal to $d = r * caRB = r * 0.01$, where *d* represents a number of pixels shift in the radial direction (see Figure 9). On a position on a distance of 100 pixels from the image center (*r* = 100), shift *d* is 1 pixel on a R (or B) color plane, which is equal to 2 pixels on the full Bayer grid.

Since $d = caRB * r$, the shift in the horizontal direction is $dx = caRB * (x - Xc)$ and in the vertical direction $dy = caRB * (y - Yc)$, where x and y represent x and y coordinates of the current pixel with respect to the top-left image position. Likewise, for each pixel, the parameter $caRB$ can be estimated as d/r. To find a better average estimate, one can average all d/r values in that image and find an average parameter $caRB$. However, the accuracy of this method is lower than the mean square error method in which, for instance, a linear fit is performed to satisfy the formula $d = caRB * r$. Correspondingly, a value of $caRB$ with a least mean-square error is estimated as:

$$caRB = \frac{\sum_i caRB_i \quad r_i}{\sum_i r_i^2},$$

wherein the sum is taken over all considered R (or B) edge pixels.

Above, a case was shown in which a 1st order approximation of LCA was used. It is, however, as mentioned, also possible to use a 3rd order LCA model, in which $f(r) = caRB_3 * r^3 + caRB_2 * r^2 + caRB_1 * r^1 + caRB_0$. The parameters $caRB$ can also be estimated using, for instance, a mean-square or some other method to obtain a better estimate of the real model of LCA. However, these calculations are much more complex and their sensitivity to outliers is larger as in the case of a 1st order approximation. This is why always some kind of data and parameters checks have to be performed to ensure a correct LCA model.

If caR, which is a LCA parameter for R color plane, is calculated, one may notice that measured data often show large spread. Spread can be caused by measurement errors, inaccuracy problems, matching wrong edges and other effects. To achieve a certain accuracy of the measurement, one depends on a sufficient amount of measurement points which statistically give a good estimate of the LCA parameters. This is why it is better to perform some statistical tests and discard data that are likely to be wrong. In a second step, additional checks are performed. As an example, one can for instance discard all measurement points that are too far from the average measurement obtained in the previous step. For instance, data that is not in the range $(caRB - 3 * \sigma \ldots caRB + 3 * \sigma)$ may be ignored. Here σ can represent a standard deviation of the measured data and *caRB* is estimated in the previous step. However, measured standard deviation can be very large, so σ may be limited by the mean value itself *(caRB).* Likewise, effectively and efficiently data can be limited between 0 and $2 * caRB$. If the sign of the shifted data is known at this step (from past measurements or lens characteristics, for instance), one can also require that only data points with the same sign as their mean value are considered, so that measurements are disregarded resulting in LCA shifts in the direction opposite to the real shift. In addition, one can demand to include a sufficient number of measurement points (for instance more than 100), to be able to reliably estimate the LCA parameter. Finally, only data that satisfy these conditions can be used to recalculate the value of *caRB.*

In a correction step, R/B data are resampled to correct for the lateral chromatic aberration shift. Lateral chromatic aberration and its 3rd or 1st order shift functions *f(r)* have been discussed before. The function *f(r)* describes a shift of the R (B) pixels with respect to the G pixel which is taken as a reference. The shift is depicted as a shift vector in Figure 14. Correspondingly, the real values of the R or B pixels at any position (x, y) are not the ones that are measured on that position but are displaced to a new location given by the shift vector. This new position is, for most of the time, not located on the existing pixel grid, so those values have to be estimated from their neighbors. For instance, in case of the bilinear interpolation, four pixels k, l, m and n around the real pixel position are taken by observing the shift vector. The integer part of the shift vector determines which four pixels to take, and fractional part determines weights w_x and w_y for the interpolation. Here, bilinear re-sampling is performed due to its simplicity. Bi-cubic or any other re-sampling is also possible, however somewhat more expensive since calculations with more pixels (for instance 16) and likewise more line memories (3 or more instead of 1) are needed.

Firstly, a LCA shift vector is calculated for each R and B pixel under examination. The vector depends on the chromatic aberration parameters *caR (caB)* and radial distance r of the pixel with respect to the optical image center (Xc, Yc). Here, x and y are pixel coordinates starting at the top left image corner and increasing to the right and towards down, respectively (see Figure 15).

It can be noted (Figure 15) that the horizontal shift can be given as

$$dx = d * cosQ = d * r_x / r = caRB * r * r_x / r = caRB * r_x = caRB * (x - Xc).$$

Similarly,

$$dy = d * sinQ = d * r_y / r = caRB * r * r_y / r = caRB * r_y = caRB * \{ y - Yc).$$

Hence, the shift vector can be represented in terms of the x and y position of the current pixel in the image avoiding calculating its radial distance r. Thus, writing the above separately for the R and B color plane, one gets (notice that caR and caB mainly have opposite sign):

$$dRx\{x, y) = caR * (x - Xc); dRy\{x, y) = caR * (y- Yc);$$
$$dBx\{x, y) = caB * (x - Xc); dBy\{x, y) = caB * \{ y - Yc).$$

In case a 3rd order LCA shift model is used, $caRB$ are now vectors with four elements:

$$caRB = [caRBz\ caRB_2\ caRB\^{}\ caRB_0],$$

and the corresponding shift vectors for a position (x, y) are:

$$dRx\{x,y) = caR_3 * \{x-Xcf+ caR_2 * \{x-Xcf + caR\^{} (x-Xc)^1 + caR_0,$$
$$dRy\{x,y) = caR_3 * \{y-Ycf+ caR_2 * \{y-Ycf + caR\^{} (y-Yc)^1 + caR_0,$$
$$dBx\{x,y) = caB_3 * \{x-Xcf+ caB_2 * \{x-Xcf + caB\^{} * (x-Xc)^1 + caB_0,$$
$$dBy\{x,y) = caB_3 * \{y-Ycf+ caB_2 * \{y-Yc)^2 + caB\^{} * (y-Yc)^1 + caB_0,$$

Here, caR_0 and caB_0 are present to accommodate a possibility that a value of LCA is not equal to zero in the optical center of the image. On the other hand, if the optical center of the lens (and hence a reference, a zero point for the LCA) does not coincide with the image center, an offset has to be introduced:

Xc = Total number of pixels (horizontal) *12* + offset (horizontal) and
Yc = Total number of pixels (vertical) *12* + offset (vertical).

As the last step, knowing all the model parameters and shift vectors, one needs to find an output pixel value which represents a real value that should have been on a position (x, y), if there was no LCA. To this purpose, various interpolation techniques can be used, for instance a bi-linear interpolation. For calculating a real pixel value that corresponds to a current pixel position, one needs to fetch surrounding four pixels k, l, m, and n (see Figure 14), given by a shift vector *(dRBx, dRBy),* for instance equal to (2.2, -2.45).

One also needs a sub-pixel position given by weights w_x and w_y. If a position of the current pixel is (x,y), the four neighboring pixels have the coordinates:

k: x +floor{dRBx{x, y)), *y + floor{dRBy{x, y)),*
l: x + floor{dRBx{x, y)) + 1, y + *floor{dRBy{x,* y)),
m: x + floor{dRBx{x, y)), y + *floor{dRBy{x,* y)) + 1,
n: x + floor(dRBx(x, y)) + 1, *y+floor(dRBy(x, y))* + 1,

and the corresponding weights are given by

$$w_x = dRBx\{x, y) - floor\{dRBx\{x, y)), \; w_y = dRBy\{x, y) - floor\{dRBy\{x, y)).$$

floor{.) is a function giving an integer part of the shift. It is equal to a first integer value smaller than its argument. In the previous example where *{dRBx, dRBy)* = (2.2, -2.45), floor(dRSx) = 2 and floor(dRSy) = -3.

Finally, bilinear interpolation function (as in Figure 2) gives an output R or B value:

$$outRB(x,y) = (1 - w_x) * (1 - w_y) * k + w_x * (1 - w_y) * l + (1 - w_x) * w_y * m + w_x * w_y * n,$$

which represents a real R (B) value that should have been on a position (x,y) if there was no LCA.

Correspondingly, all values of R and B pixels are recalculated to correct for effect of LCA, and good color separation (finding a R, G and B pixel value at each location) can be performed afterwards. However, this technique is also applicable when R, G and B pixel values already exist on all grid positions, but LCA deteriorates the image quality.

Claims

1. A method for detection (10) and correction (40) of a lateral chromatic aberration shift of at least one of a red (R) and a blue (B) color plane in relation to a green (G) color plane in digital image data, the method including for at least one region of the digital image data:

   a) determining (3) a first edge in the red (R) and/or blue (B) color plane;

   b) determining (3) a second edge in the green (G) color plane or in a color plane (GonR, GonB) derived (1) from the green (G) color plane, at least one second edge corresponding to the at least one first edge;

   c) determining (6) a shift between the first and second edges; and

   d) correcting (40) the lateral chromatic aberration shift by shifting the red (R) and/or blue (B) color plane in the image region based on the shift between the first and second edges.

2. A method according to claim 1, wherein determining (3) the edges in step a) and/or in step b) includes determining (3) luminance edges and/or edges with a magnitude exceeding a threshold.

3. A method according to claim 1 or 2, wherein determining (3) the edges in step a) and/or in step b) includes determining (3) isolated edges to assure that the second edge corresponds to the first edge.

4. A method according any one of the preceding claims, wherein determining (3) the edges in step a) and/or in step b) includes determining (3) the edges after using a Laplacian operator and/or checking for a set of conditions.

5. A method according any one of the preceding claims, wherein the digital image data are acquired by a pixel sensor (100), especially a pixel sensor (100) including a Bayer pattern, and wherein a color plane (GonR, GonB) is derived (1) from the green (G) color plane by matching the green (G) color plane with red (R) and/or blue (B) pixel positions of the pixel sensor (100).

6. A method according any one of the preceding claims, wherein determining (6) the shift in step c) includes determining (3) a radial distance of the edges based on a horizontal and/or a vertical distance of the edges and/or on a correction factor based on a position of the image region in the image data and orientation of the edge.

7. A method according any one of the preceding claims, wherein a model function *(f(r))* describing the lateral chromatic aberration shift is used and parameters *(caRB)* of the model function *(f(r))* are used to correct the LCA shift of the R and/or B color plane.

8. A method according to any one of the preceding claims, wherein in step d) correcting (40) the lateral chromatic aberration shift in step d) includes applying a correction function *(outRB(x, y))* based on the shift between the first and second edges and/or on a model function *(f(r))* describing the lateral chromatic aberration shift to generate corrected image data.

9. A method according any one of the preceding claims, further including filtering (2), especially low-pass filtering, the red (R), the blue (B) and/or the green (G) color plane and/or a color plane (GonR, GonB) derived (1) from the green (G) color plane.

10. An image processing device for detection (10) and correction (40) of a lateral chromatic aberration shift of at least one of a red (R) and a blue (B) color plane in relation to a green (G) color plane in digital image data, the method including, operable for at least one region of the digital image data:

a) means for determining (3) a first edge in the red (R) and/or blue (B) color plane;

b) means for determining (3) a second edge in the green (G) color plane or in a color plane (GonR, GonB) derived (1) from the green (G) color plane, the at least one second edge corresponding to the at least one first edge;

c) means for determining (6) a shift between the first and second edges; and

d) means for correcting (40) the lateral chromatic aberration shift by shifting the red (R) and/or blue (B) color plane of the image region.

11. A computer program product adapted to be executed in an image processing device according to claim 9 and adapted, when executed, to perform a method according to any one of claims 1 to 8.

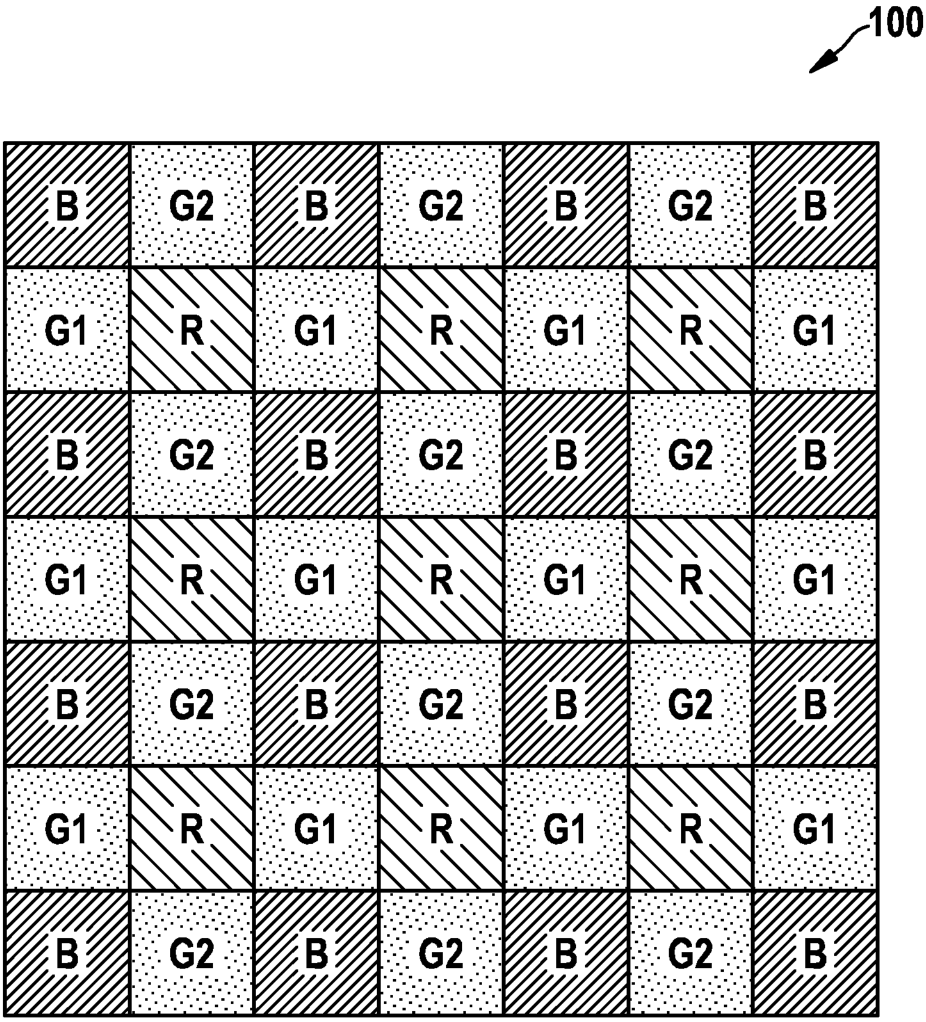

Fig. 1
(Stand der Technik)

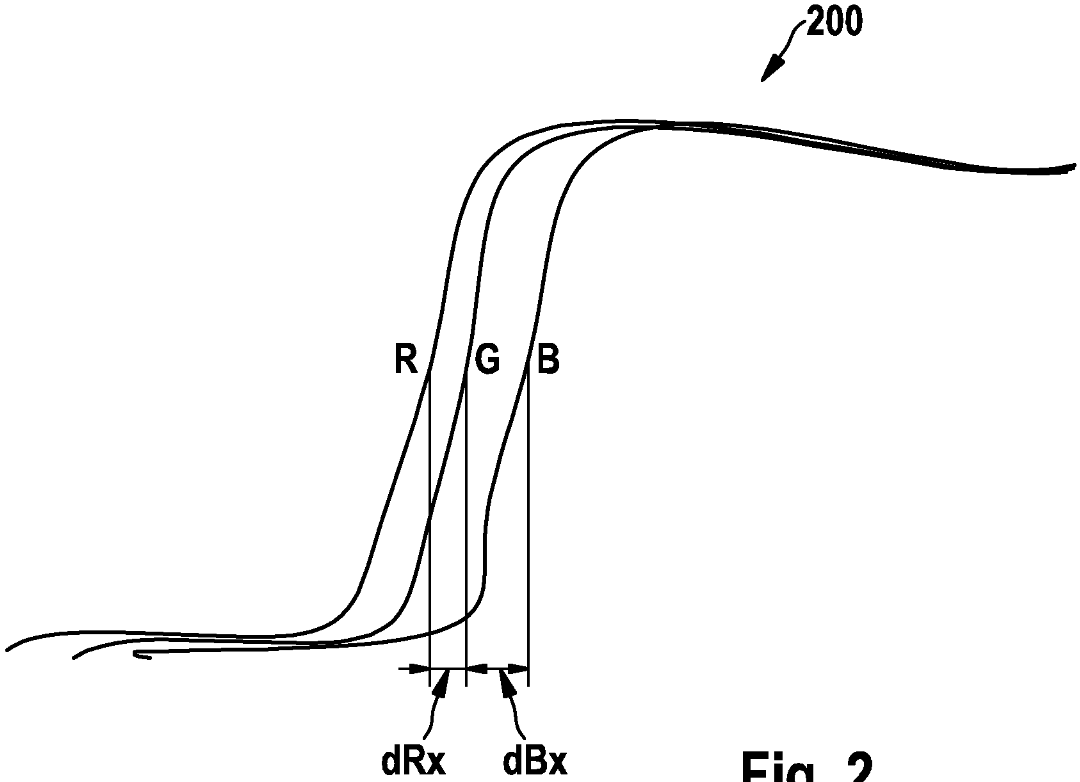

Fig. 2

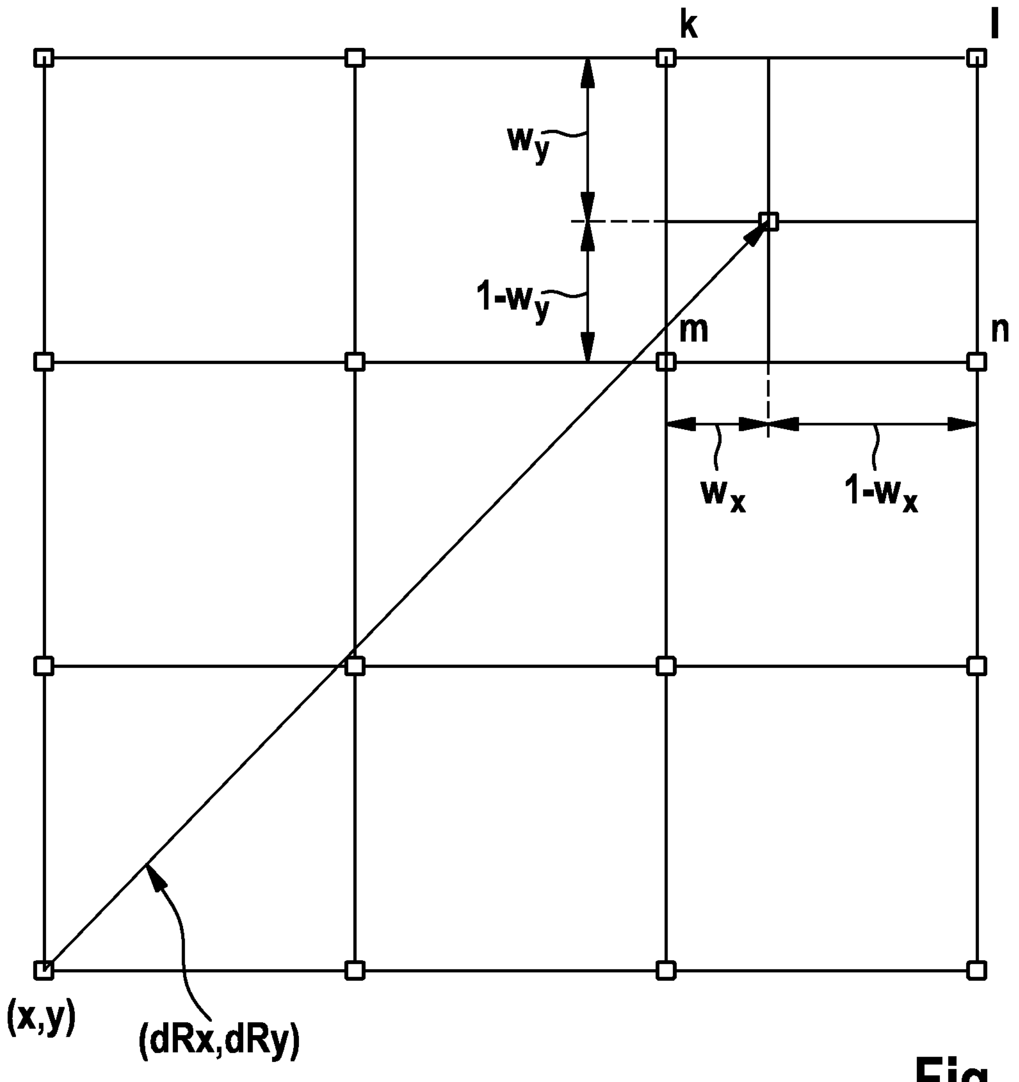

Fig. 3

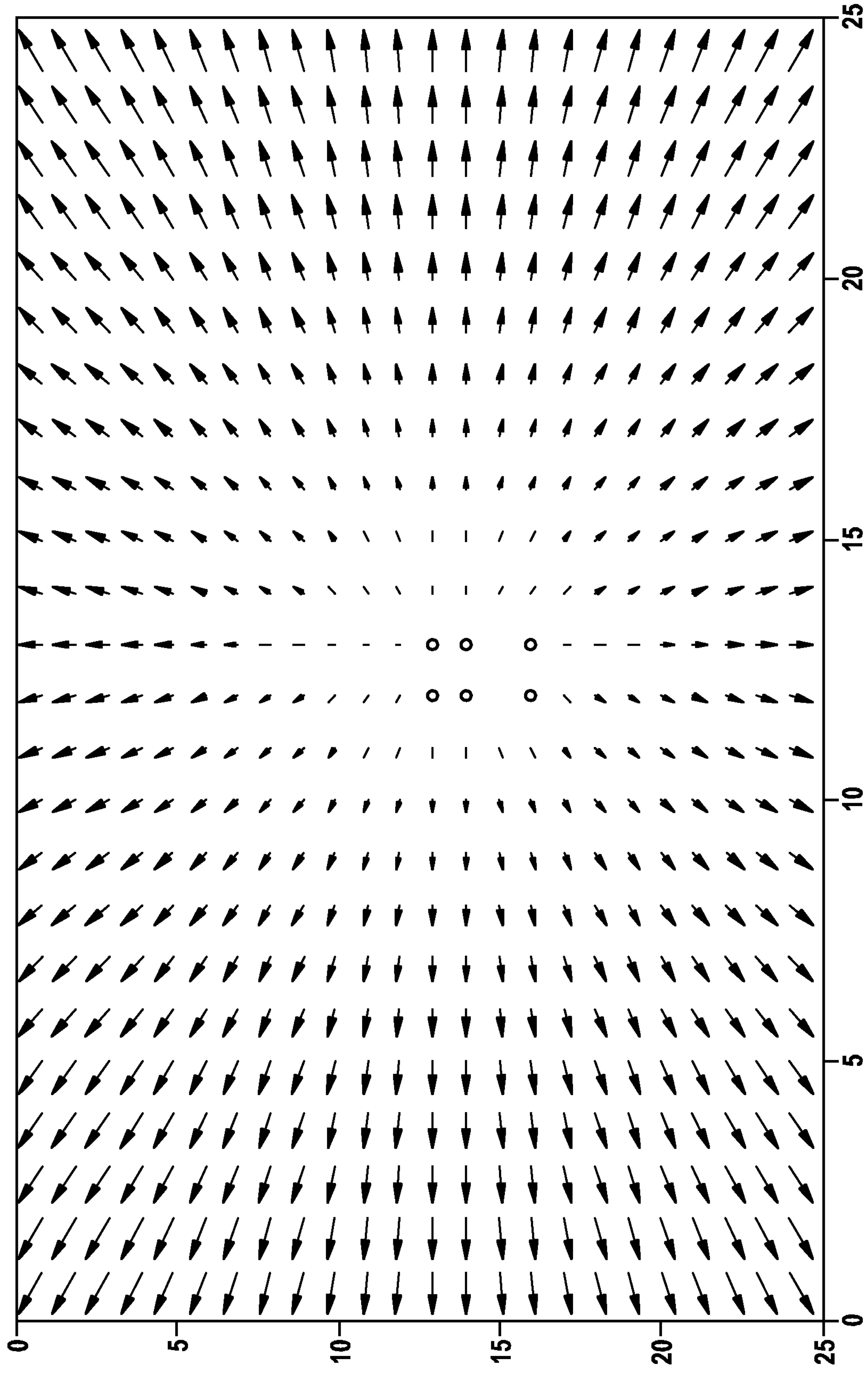

Fig. 4

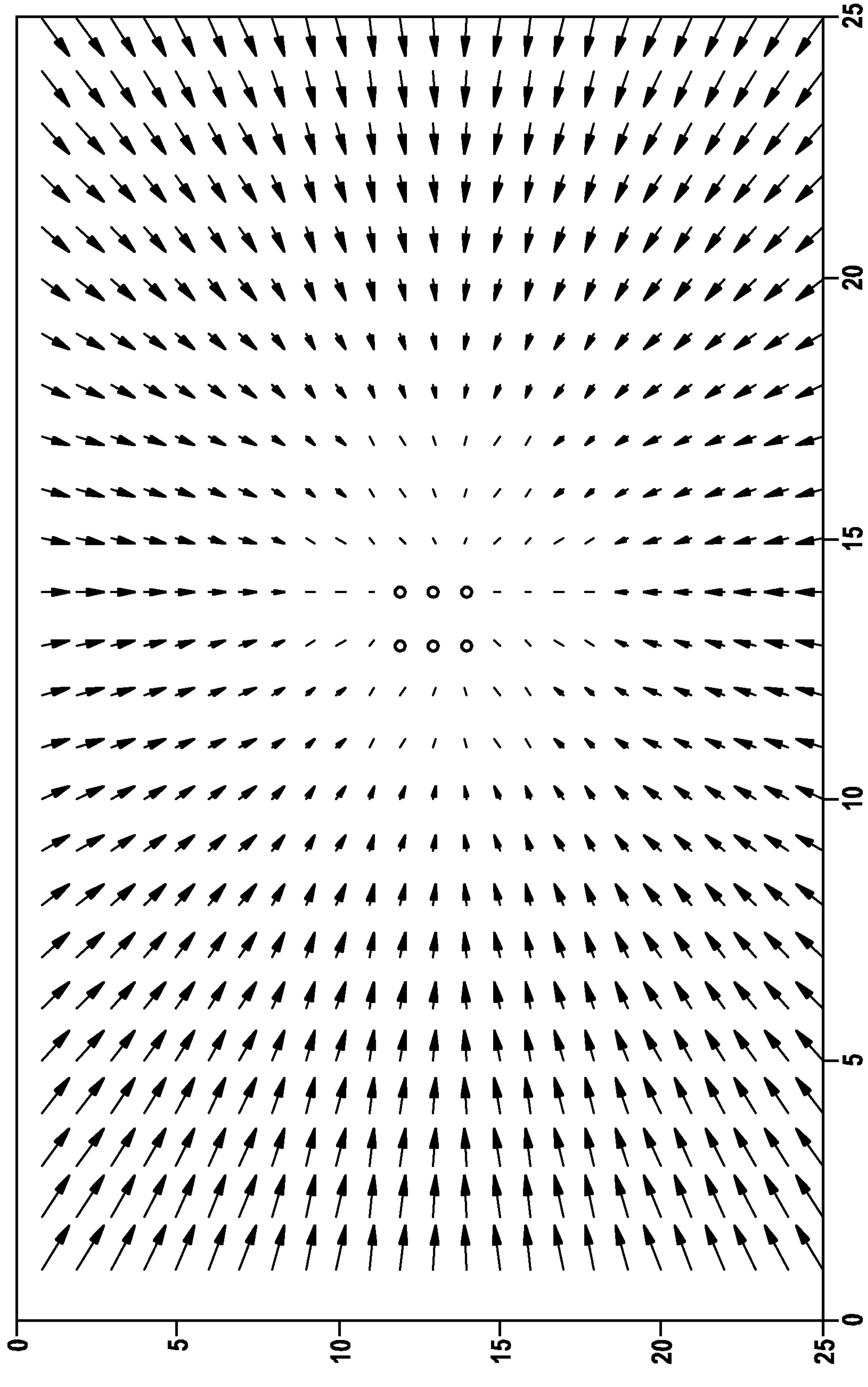

Fig. 5

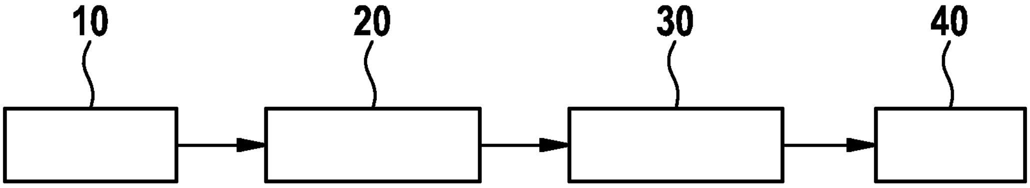

Fig. 6

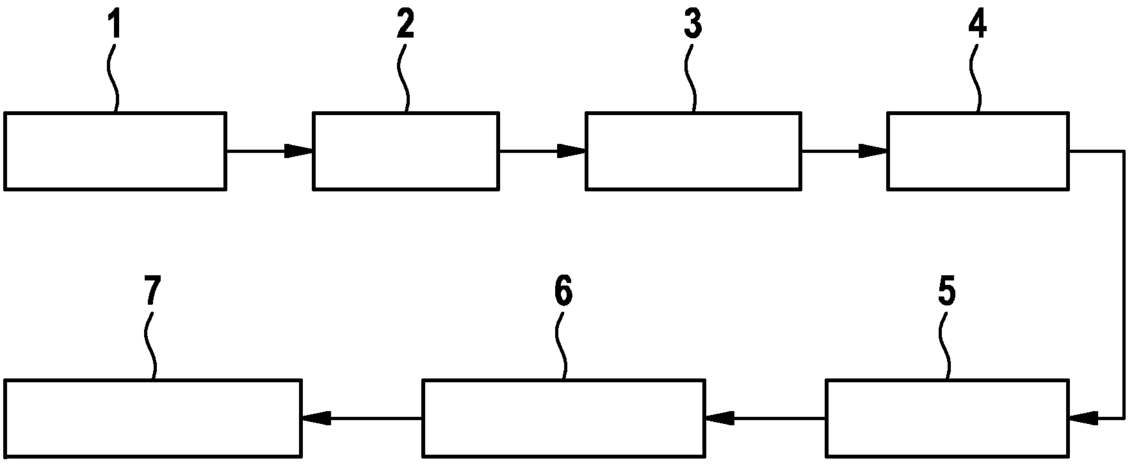

Fig. 7

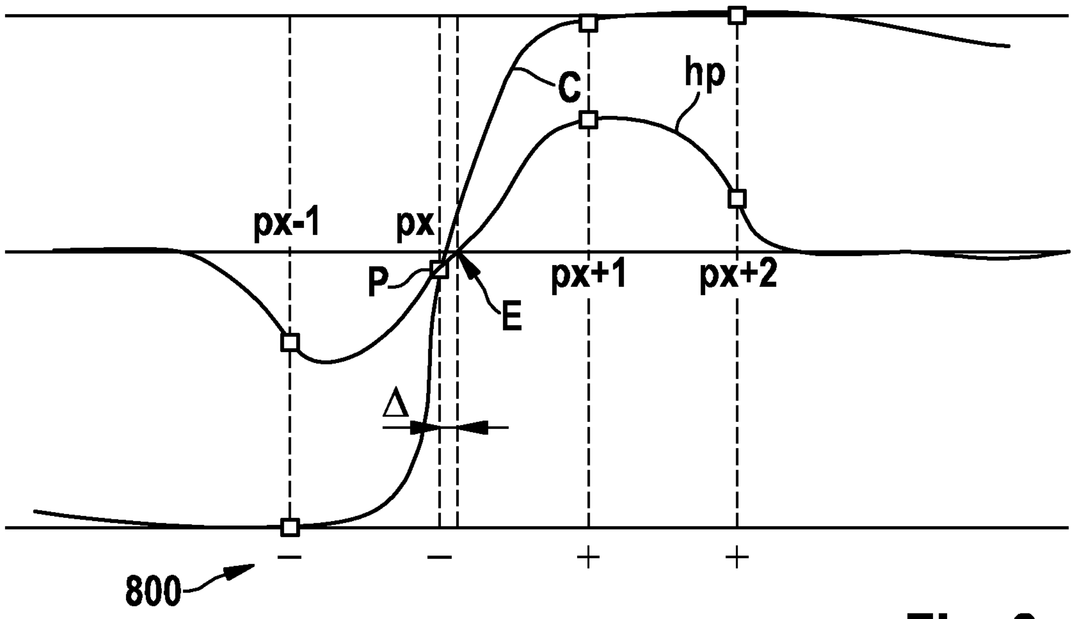
hp
C
px-1
px
P
E
px+1
px+2
Δ
800

Fig. 8

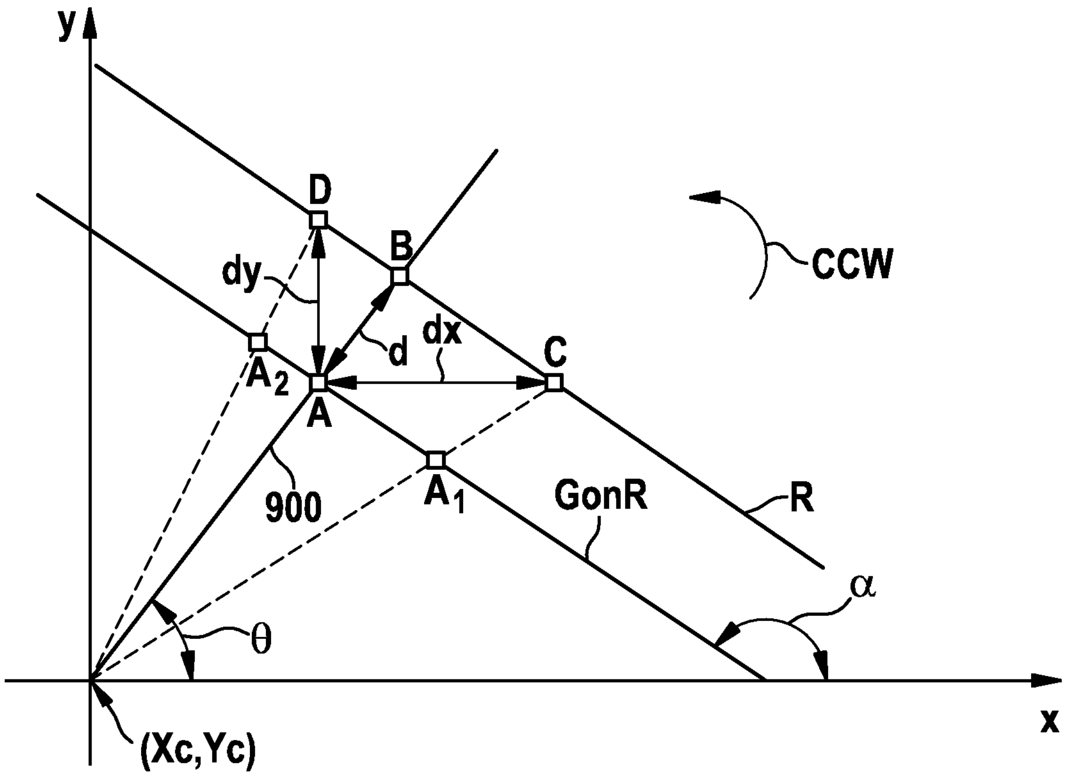
y
D
B
CCW
dy
d
dx
C
A2
A
A1
900
GonR
R
α
θ
x
(Xc,Yc)

Fig. 9

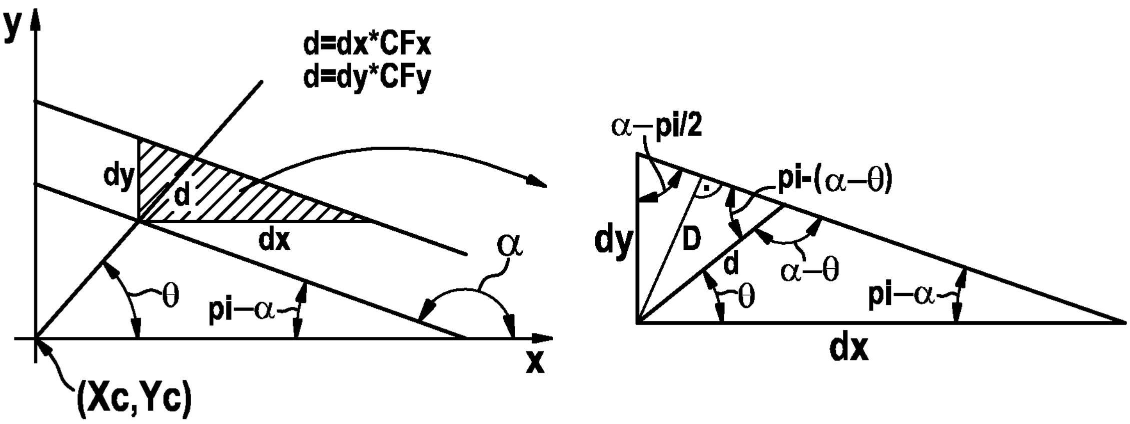
y
d=dx*CFx
d=dy*CFy
dy
d
dx
α
θ
pi−α
x
(Xc,Yc)
α−pi/2
pi-(α−θ)
dy
D
d
α−θ
θ
pi−α
dx

Fig. 10

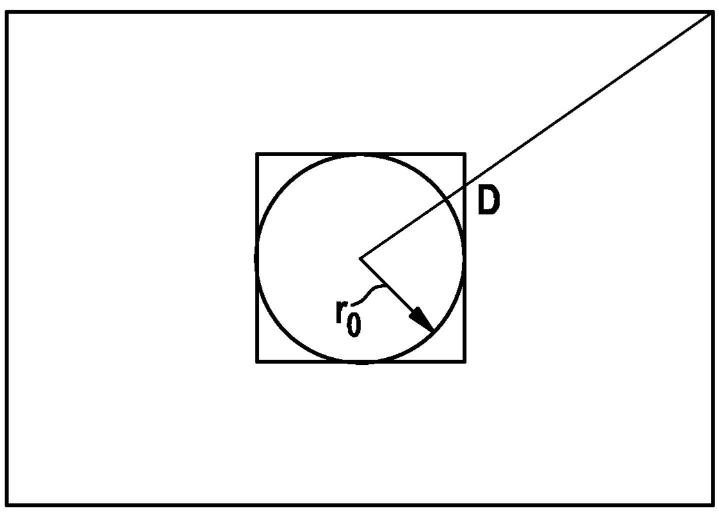
D
r_0

Fig. 11

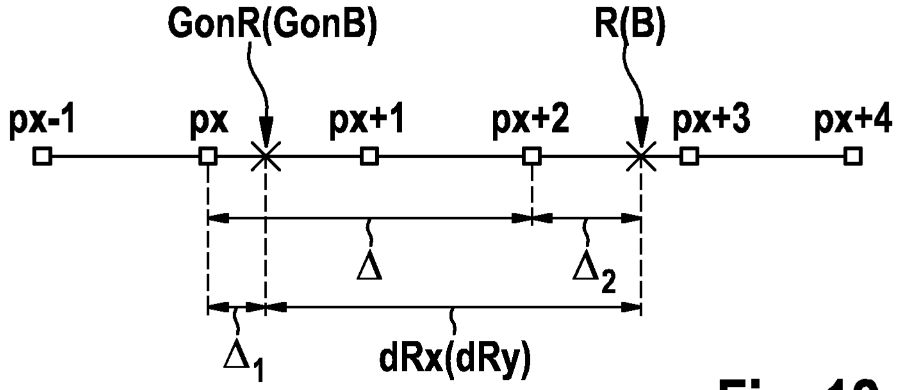
GonR(GonB)
R(B)
px-1
px
px+1
px+2
px+3
px+4
Δ
Δ2
Δ1
dRx(dRy)

Fig. 12

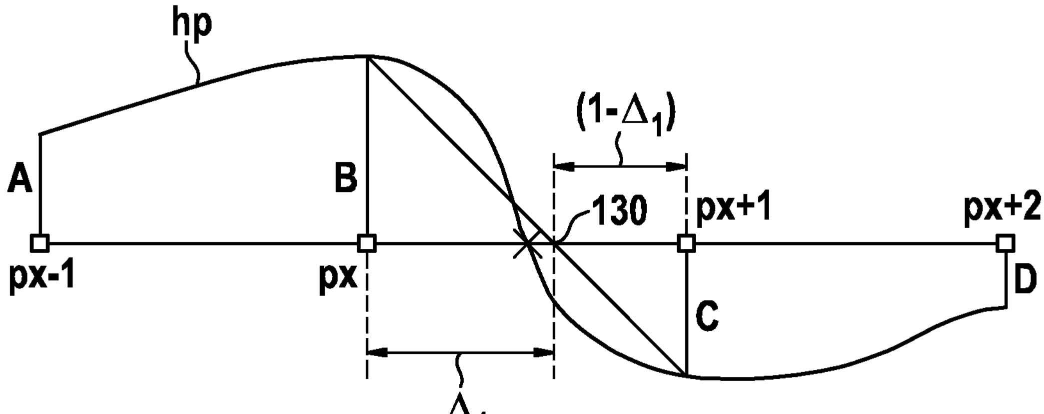
hp
(1-Δ1)
A
B
130
px+1
px+2
px-1
px
D
C
Δ1

Fig. 13

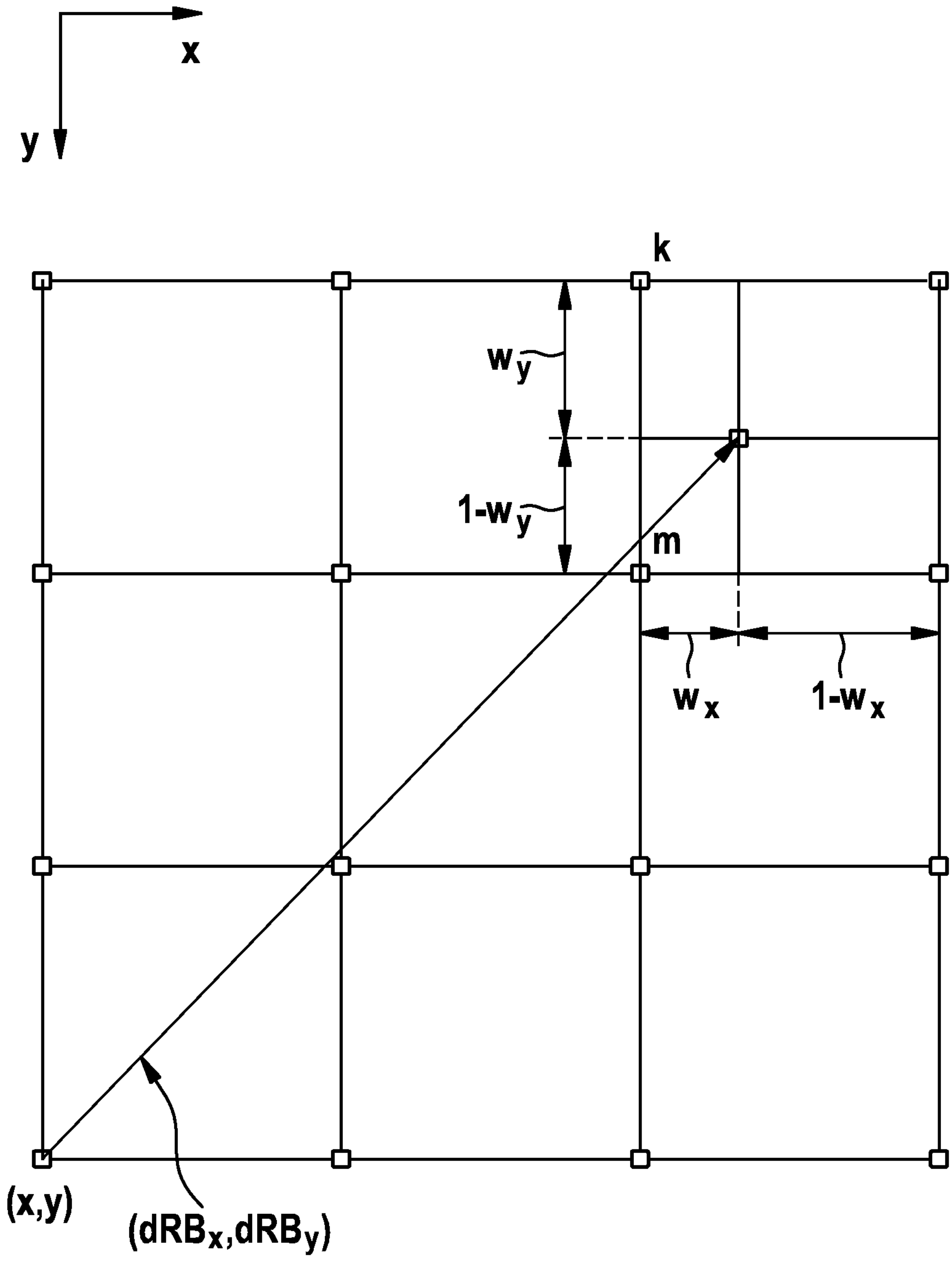

Fig. 14

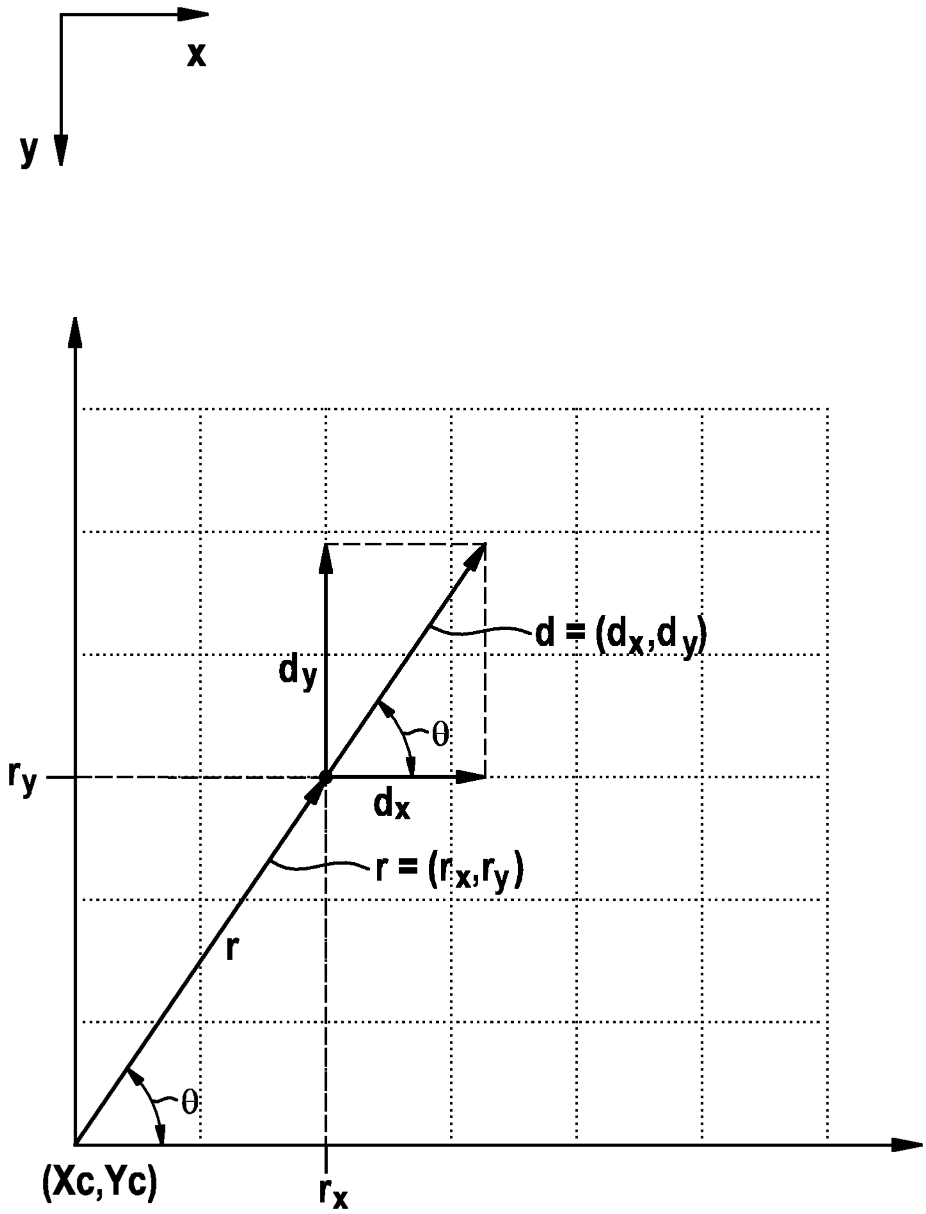

Fig. 15

INTERNATIONAL SEARCH REPORT

International application No
PCT/E P20 10/060367

A. CLASSIFICATION ,OF SUBJECT MATTER
INV. H04N9/04 H04N9/07 H04N5/357
ADD.

According to International Patent Classification (IPC) or to both national classification and IPC

B. FIELDS SEARCHED

Minimum documentation searched (classification system followed by classification symbols)
H04N

Documentation searched other than minimum documentation to the extent that such documents are included in the fields searched

Electronic data base consulted during the international search (name of data base and, where practical, search terms used)

EPO-Internal

C. DOCUMENTS CONSIDERED TO BE RELEVANT

Category"	Citation of document, with indication, where appropriate, of the relevant passages	Relevant to claim No.
X Y	EP 1 746 846 A1 (NIPPON KOGAKU KK [JP]) 24 January 2007 (2007-01-24) * abstract paragraphs [0037] - [0050]; figure 1 figures 10,16	1,2,5-11 3,4
Y	EP 0 878 970 A2 (MATSUSHITA ELECTRIC IND CO LTD [JP]) 18 November 1998 (1998-11-18) * abstract page 2, lines 44-53 page 8, line 16 - page 10, line 29 page 10, lines 30-39	3,4

-/--

[X] Further documents are listed in the continuation of Box C.

[X] See patent family annex.

* Special categories of cited documents :

"A" document defining the general state of the art which is not considered to be of particular relevance

"E" earlier document but published on or after the International filing date

"L" document which may throw doubts on priority claim(s) or which is cited to establish the publication date of another citation or other special reason (as specified)

"O" document referring to an oral disclosure, use, exhibition or other means

"P" document published prior to the international filing date but later than the priority date claimed

"T" later document published after the international filing date or priority date and not in conflict with the application but cited to understand the principle or theory underlying the invention

"X" document of particular relevance; the claimed invention cannot be considered novel or cannot be considered to involve an inventive step when the document is taken alone

"Y" document of particular relevance; the claimed invention cannot be considered to involve an inventive step when the document is combined with one or more olher such documents, such combination being obvious to a person skilled in the art.

"&" document member of the same patent family

Date of the actual completion of the international search	Date of mailing of the international search report
6 December 2010	21/12/2010

Name and mailing address of the ISA/	Authorized officer
European Patent Office, P.B. 5818 Patentlaan 2 NL- 2280 HV Rijswijk Tel. (+31-70) 340-2040, Fax: (+31-70) 340-3016	Mao, Pauline

INTERNATIONAL SEARCH REPORT

International application No
PCT/EP2010/060367

C(Continuation). DOCUMENTS CONSIDERED TO BE RELEVANT

Category*	Citation of document, with indication, where appropriate, of the relevant passages	Relevant to claim No.
X	US 2008/291447 A1 (VAKRAT DUDI [IL] ET AL) 27 November 2008 (2008-11-27) cited in the application	1,8,10, 11
A	* abstract; figures 1,2,5 paragraphs [0020] - [0023]; figure 3 paragraphs [0029] - [0030]; figure 4 -----	5-7
A	US 2008/298678 A1 (KANG SING BING [US]) 4 December 2008 (2008-12-04) * abstract paragraphs [0005] - [0006] paragraph [0035]; figures 5-6 paragraphs [0043] - [0044]; figure 7 paragraph [0058] paragraphs [0059] - [0077]; figure 13 -----	1,5-8, 10,11

INTERNATIONAL SEARCH REPORT

Information on patent family members

International application No
PCT/EP2010/060367

Patent document cited in search report	Publication date	Patent family member(s)	Publication date
EP 1746846 A1	24-01-2007	WO 2005101854 A1	27-10-2005
		US 2007116375 A1	24-05-2007
EP 0878970 A2	18-11-1998	CN 1200625 A	02-12-1998
		JP 11055695 A	26-02-1999
		US 2001030697 A1	18-10-2001
US 2008291447 A1	27-11-2008	NONE	
US 2008298678 A1	04-12-2008	NONE	